Electrochemical Preparation and EPR Studies of Lithium Phthalocyanine. Part 2: Particle-Size-Dependent Line Broadening by Molecular Oxygen and Its Implications as an Oximetry Probe

Govindasamy Ilangovan, Jay L. Zweier, and Periannan Kuppusamy*

The EPR Center and Division of Cardiology, Department of Medicine, Johns Hopkins University, School of Medicine, 5501 Hopkins Bayview Circle, Baltimore, Maryland 21224

Received: April 13, 2000; In Final Form: June 5, 2000

As an extension of our previous report (Ilangovan, G.; Zweier, J. L.; Kuppusamy, P. *J. Phys. Chem. B* **2000**, *104*, 4047) on the synthesis and characterization of lithium phthalocyanine (LiPc) as an electron paramagnetic resonance (EPR) oximetry probe, we investigated the mechanism of the effect of molecular oxygen on the EPR spectrum of the LiPc. Electrochemical preparation of LiPc under potentiostatic conditions (+0.4 V) yielded microcrystals that showed extremely narrow (peak-to-peak width < 10 mG) EPR spectrum under anoxic conditions. In this study it is observed that the peak-to-peak width is particle-size-dependent. The total EPR line shape is observed to be a composite of several components present in the microcrystalline powder. Deconvolution of the composite shape showed the presence of at least three major components corresponding to different crystal sizes in the bulk sample. The mechanism of EPR line broadening of LiPc in the presence of molecular oxygen is entirely different from that of dissolved paramagnetic probes such as nitroxides. The EPR line width variations observed in the present case are interpreted using a two-spin state model, namely mobile and fixed spin states, originally proposed for *trans*-polyacetylene. Further, the sensitivity of EPR line width to oxygen partial pressure (pO_2), measured as the slope of EPR line width of LiPc versus pO_2 plot, is higher compared to previously reported values. The higher sensitivity is due to smaller crystal size, wherein the molecular oxygen can easily diffuse into microchannels of LiPc crystals. At higher pO_2 values, the oxygen-induced EPR line broadening shows a saturation behavior, which is quantitatively interpreted from the dynamics of the two-spin model. Thus, the oxygen sensitivity of the LiPc particles is strongly dependent on the size of individual particles. The results will enable selective synthesis and control of LiPc probe suitable for a given oximetry application.

Introduction

Accurate quantification of molecular oxygen concentration in chemical and biological systems is an important area of research. Since oxygen utilization is associated with normal metabolic control, any abnormal variation in the supply of oxygen is closely linked to many of the major types of pathology like ischemic heart disease, reperfusion injury or even oxygen toxicity.[1] Also therapeutic regimens such as chemo- or radiotherapy in cancer treatment are very sensitive to the quantity of oxygen in the region of the tumor.[2] Thus it is highly advantageous to be able to quantify local tissue oxygenation in some units of partial pressure (pO_2, mmHg) or concentration (μM), and to correlate this with pathophysiology or treatment outcome. In many chemical/biochemical systems, real-time monitoring of oxygen is important since many of the photosynthetic studies[3] and photosensitized oxygen consumption or release[4] reveal some of the crucial mechanistic information or the active site involved in the photosynthetic processes.

In recent years electron paramagnetic resonance (EPR) spectroscopy has been shown to be useful for in situ or in vivo measurements of oxygen (oximetry) in many biochemical and biological systems.[5] The EPR technique provides real-time, noninvasive, and nonperturbing measurements of oxygen. Molecular oxygen is paramagnetic and it has two unpaired electrons in the ground state. Nevertheless, it cannot be directly detected by EPR at ambient conditions due to fast relaxation of the excited state, resulting in broad and low-amplitude EPR spectrum. However, it can be measured indirectly from the oxygen-induced EPR line broadening of other suitable paramagnetic probes in the system. This technique is known as EPR oximetry.[5] The EPR oximetry technique is based on the principle of Heisenberg spin−spin exchange between molecular oxygen and another spin probe. This exchange will shorten the relaxation time of the spin probe causing an increase in the peak-to-peak width in the first derivative EPR spectrum. In systems wherein the spin probe and molecular oxygen are freely tumbling, the effect of oxygen on the probe spin can be quantified in terms of bimolecular collision frequency ω, which is related to the oxygen concentration as defined by the classic Smoluchowski equation:[5]

$$\omega = 4\pi R(D_{O_2} + D_{SL})[O_2] \quad (1)$$

where R is the interaction distance, D_{O_2} and D_{SL} are the diffusion coefficients of oxygen and the spin probe, respectively, and $[O_2]$ is the concentration of the oxygen. The peak-to-peak line width (LW) caused by the molecular oxygen is directly proportional to the collision rate. Thus a plot of LW vs $[O_2]$ is expected to be linear and hence the relationship can be used to obtain any

* Author to whom correspondence should be addressed: Phone: 410-550-3229. Fax: 410-550-2448. E-mail: kuppu@jhmi.edu.

10.1021/jp0013863 CCC: $19.00
Published on Web 09/13/2000

unknown oxygen concentration. Using this principle, many magnetic resonance imaging techniques including nuclear magnetic resonance imaging,[6] Overhauser magnetic resonance imaging,[7] and EPR imaging[8] have been developed to enable spatially resolved mapping of oxygen concentration.

The EPR oximetry is unique in its potential for high-sensitivity oxygen measurements. However, its application has been limited by the difficulties in preparing suitable spin probes that are capable of providing high-resolution oxygen data over a wide variety of oxygenation conditions. Though there are a variety of soluble EPR spin probes, such as nitroxides, suitable for oximetry, they lack in sensitivity especially in the most desired pathophysiological oxygen range (0−76 mmHg).[9] Alternatively, many solid-state probes with relatively high spin density ($10^{18}-10^{19}$ spins/g) such as charcoal,[10] fusinite,[11] and India ink[12] have been developed. Similarly many synthetic materials such as lithium phthalocyanine (LiPc), chars, etc., have also been recognized as highly sensitive probes.[13,14] The LiPc, in particular, has several advantages including extremely sharp EPR absorption line, very short response time, and reusability for repeated measurements.[13] However, synthesis of LiPc in a pure and desirable oxygen-sensitive form has been a critical problem and challenge in this field. Recently we reported a reliable and reproducible electrochemical preparative procedure to obtain oxygen-sensitive LiPc microcrystalline powder. Important issues including the effect of preparative conditions on the resulting material and the influence of deposition mechanism on crystal structure were investigated using cyclic voltammetry, chronoamperometry, X-ray diffraction (XRD), and high- and low-frequency EPR measurements.[13e]

However, critical questions remain regarding the mechanism of oxygen-dependent line broadening and the effect of preparative conditions on this mechanism. Therefore, the goal of the present work was to characterize the mechanistic basis of the effect of molecular oxygen on the EPR line shape of the LiPc. Marked differences in the oximetry behavior of the LiPc microparticles were observed compared to the previous reports: (i) a nonlinear oxygen response curve (LW vs pO_2) unlike the linear curve reported for single-crystal measurements,[13a] and (ii) a higher slope in the linear region of the response curves. These two issues are addressed in the present paper by proposing a two-spin state model. The same model is also used to discuss the mechanism of sample size-dependent line broadening.

Experimental Details

Electrochemical Preparation. Electrochemical preparation of LiPc in microcrystalline form was carried out as described in our previous report.[13e] Dilithium phthalocyanine (Aldrich) was oxidized to the monolithium LiPc radical as

$$Li_2Pc \xrightarrow[\text{at 0.4 V}]{\text{electrolysis}} LiPc\downarrow + Li^+ + e^-$$

The electrodeposition was carried out using a potentiostatic technique at a constant potential of +0.4 V (Ag/AgCl) using a platinum-mesh working electrode (BAS, West Lafayette, IN) in acetonitrile containing tetrabutylammonium perchlorate (ICN Biochemicals, Aurora, OH) as the supporting electrolyte. Constant stirring was applied during the electrolysis. The resulting microcrystalline powder was removed by filtration from the electrolytic solution. The powder was characterized using optical microscopy and X-ray diffraction (XRD) to confirm that it was predominantly crystalline in nature. Since LiPc is known to exist in three polymorphic forms, namely, α form, β form, and x form, the crystalline powder was subjected to XRD analysis. The XRD patterns confirmed that the material was predominantly the oxygen-sensitive x form.[13e] The optical microscopic results showed that the crystals were needle-shaped and present in different sizes ranging from 10 to 80 μm. A small fraction of the amorphous form of LiPc was also seen in the micrographs.

Measurement and Analysis of EPR Spectrum. EPR measurements were carried out at X-band, 9.78 GHz, using a Bruker ER 300 spectrometer with TM_{110} microwave cavity. Data acquisition and analysis were performed using an IBM-compatible personal computer interfaced to the spectrometer. Instrument control, data acquisition, and processing were performed using SPEX, a personal computer software developed in our laboratory. Since the peak-to-peak width of the LiPc spectrum was extremely small (anoxic width < 10 mG), low modulation amplitude (<5 mG) at a frequency of 12.5 kHz was used in order to avoid any instrumental distortion to the spectrum. Also, since the sample is highly saturable,[13e] the measurements were performed using very low microwave powers (20−50 μW). The first derivative EPR spectra were integrated and subjected to area and line-shape analysis. The line shapes were analyzed as pure Lorentzian and Voigt (combination of Gaussian and Lorentzian functions) lines using commercial software PeakFit (SPSS, Chicago, IL). In the fitting of the data, both the full width at half-maximum and the amplitude were treated as variables and optimized for all the individual spectra under the envelope. The best fit was assessed from minimum χ-square and the maximum correlation coefficient. All the simulations were carried out by user-defined functions (transforms) in SigmaPlot (SPSS, Chicago, IL).

EPR Oximetry Studies. A known quantity of the sample was encapsulated in a 0.8 mm diameter gas-permeable Teflon tube and sealed at both the ends as described previously.[13e] Desired compositions of oxygen and nitrogen gas mixtures were used by mixing oxygen or air with nitrogen using a precalibrated gas-flow meter (Cole-Parmer, IL). The gas mixture from the flow meter was passed through a gas-impermeable silicone tube into the 3.0 mm Quartz EPR tube containing the LiPc encapsulated gas-permeable Teflon tube. All measurements were carried out after equilibrating the sample with the gas for at least 10 minutes.[13e] The flow rate of the mixture was 2000 mL/min and the partial pressure of oxygen was calculated from its ratio to the total flow. The total pressure inside the EPR tube was maintained at 760 mmHg (atmospheric pressure), since the other end of the EPR tube was opened to the atmosphere. For low oxygen partial pressures, gas cylinders containing air (21% oxygen) and pure nitrogen were used.

Results and Discussion

Effect of Particle Size on the EPR Spectrum of LiPc Crystals. An EPR spectrum obtained from LiPc crystalline powder under anoxic conditions (in the presence of 100% nitrogen) is shown in Figure 1. The spectrum is extremely sharp with a peak-to-peak width about 10 mG. Also the spectrum shows some unusual line-shape characteristics. It shows a small asymmetry, which may be due to microcrystallites that are not randomly distributed[15] and thus resulting in a small influence of anisotropic g value. The spectrum also shows an unusual shape in the wings. This shape cannot be attributed to the field-dependent magnetic resonance absorption[16] for the following reason. If this would have been the case the resonant frequency of the cavity would change and subsequently the EPR spectrum should be different when recorded with automatic frequency control "on" and "off", as previously suggested.[16] However, in

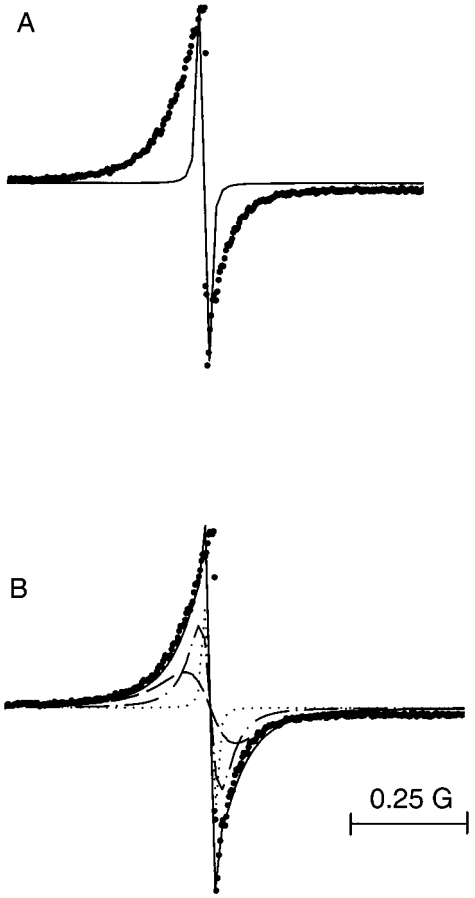

Figure 1. An anoxic EPR spectrum obtained from a microcrystalline powder sample of LiPc, prepared by potentiostatic electrochemical deposition at +0.4 V. The solid points are the experimental data and the lines are simulated data using a Lorentzian function. (A) Experimental (•) and simulated (−−) spectrum corresponding to 10 mG peak-to-peak width. Spectrometer/experimental conditions: microwave frequency, 9.7881 GHz; modulation amplitude, 2.2 mG; modulation frequency, 12.5 kHz; microwave power, 25 μW; scan time, 4.9 s. (B) Experimental spectrum (•) and calculated spectra (....), (- - -), (−•−) using peak-to-peak widths and relative contributions as shown in Table 1. The fitting parameters were obtained using eq 3 as described in the text. The composite spectrum, which is a sum of the three simulated spectra, is shown as a solid line in (B**)**.

the present work, we did not find any difference in the EPR spectral shape in either condition. Thus the shape seems to be a true characteristic of the material under study. The shape of the signal cannot be adequately fit with a single Lorentzian line shape with 10 mG peak-to-peak separation as illustrated in Figure 1A. The experimental shape showed rather narrow peak-to-peak width, but large width at half-maximum. This is likely due to the presence of different-sized crystallites in the microcrystalline powder, which might give EPR spectra with different line widths. Recently, it was observed in the case of electrodeposited LiPc thin films that with increasing the crystallite size and increasing unidirectional order in the films, the EPR line width progressively decreased.[13d] Thus the observed EPR spectrum might be a composite of lines with different widths. The observation of the size-dependent EPR line widths can be rationalized on the basis of the crystallographic packing.

The LiPc crystallizes in the form of highly ordered one-dimensional packing of the molecules. Each unit cell has four stacks and in the present case (x-form) the planar LiPc molecules are stacked exactly vertically on each other.[17] The interplanar distance (3.24 Å) is significantly smaller than the van der Waals value (3.4 Å), and thus will result in a strong intrastack spin−

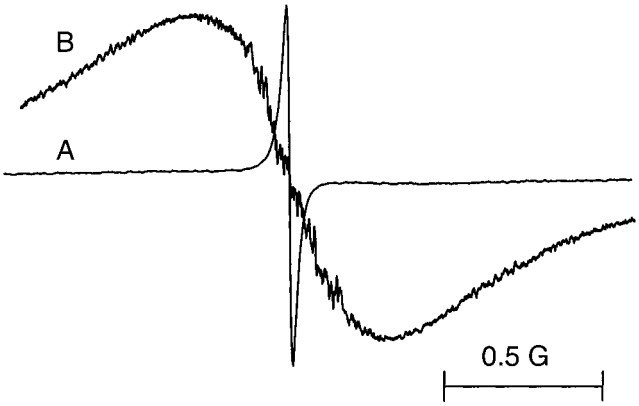

Figure 2. Effect of temperature on the EPR spectrum of LiPc microcrystalline particles. (A) EPR spectrum measured at 300 K and (B) EPR spectrum measured at 77 K. The instrument settings were as in Figure 1. The spectrum at 300 K showed an exchange-narrowed peak-to-peak line width of 10 mG, while that 77 K showed a line width of 650 mG indicating that the exchange is prevented to a significant level at low temperature

spin exchange (spin diffusion) leading to sharp EPR line shapes.[17] The occurrence of spin exchange in the LiPc crystals was confirmed by low-temperature studies. The EPR spectrum of the LiPc measured at liquid nitrogen temperature (77 K) showed a line width of 650 mG (Figure 2). This suggests that the exchange is prevented to a significant level at the low temperature.[18] In exchange coupled spin systems, there are two types of spins, namely mobile and the fixed spins, in the bulk at any given temperature. Accordingly, two superimposed EPR lines, a broad one corresponding to the fixed spins and a sharp one corresponding to the diffusing spins, are expected. However, in the present case only a single EPR line is observed, even though it involves intermolecular spin exchange. This single line is explained as due to the occurrence of a fast interchange between the fixed and mobile spin species at a defined frequency, as proposed for *trans*-polyacetylene.[19] However, the frequency of such a spin interchange between the fixed and mobile spin is independent of their ratio. As a consequence, only a single line is observed at all mobile-to-fixed spin-state ratios. However, the line width of the single line can vary depending on the ratio of the spins.

The extent or efficiency of spin exchange at room and higher temperatures depends on the packing efficiency or the crystal size. Accordingly, narrowing of the signal is expected to be most efficient in larger crystals of macroscopic size and much less in microcrystals.[13d] Any defect present in the crystal can perturb the spin mobility and trap the mobile spin into a fixed spin leading to EPR line broadening.[18] Thus, at room and higher temperatures both mobile and fixed spin states coexist and their relative magnitude depends on factors such as defect concentration, spin dynamics, etc. The line width (LW) is related to the spin−spin exchange integral, J, as follows:

$$\mathrm{LW} \propto J^{-n} \qquad (2)$$

where n is a dimensionality factor that depends on the nature of packing. For a three-dimensional spin-exchange system, n will be 1, whereas for systems with one-dimensional exchange coupling n will be 0.5. The x form of LiPc has previously been shown to be a one-dimensional spin system.[17] In both cases, line width decreases as the exchange integral increases. The maximum line width is observed in the absence of spin exchange (where $J = 0$).The exchange integral J, which is an indirect measure of the concentration of the mobile spins, depends on

TABLE 1: Peak-to-peak Width (LW) and Composition of the Major Components and Their Oxygen Responsivity Data Obtained from the Composite Spectra

	anoxic condition ($pO_2 = 0$)		oxygen responsivity	
components[a]	LW (mG)	intensity (% of total)	m (mG/mmHg)	ω/ω_0[b]
a	10	3.09	7.11	1.00
b	30	15.03	13.50	1.00
c	70	81.87	23.62	1.00

[a] See Figure 1 for details. [b] Since the oxygen response curve was linear in the region of pO_2 that was used for fitting, the ω/ω_0 was defined as 1 in the analysis.

the crystal size. For one-dimensional crystals such as LiPc, the relative area in the edges to the bulk will increase as the size of the crystal decreases. On the other hand, the edges of one-dimensional solids act as a barrier or defect. Subsequently, the defect concentration also depends on the size of the crystal. Thus the ratio of the mobile to fixed spin concentration will depend on the size of the crystal. A microscopic examination of the LiPc material prepared in the present study showed crystals of various sizes in the range of 10−80 μm.[13e] Thus in the present case, a distribution of J values is expected, subsequently leading to a composite spectrum consisting of many individual lines with different widths. Optical microscopic evidences also showed the presence of a small fraction of amorphous material. Consistently, there was also a small fraction of absorption, with LW about 650 mG (not shown in Figure 1). The maximum line width, 650 mG, observed is attributed to the amorphous material with $J = 0$. On the other hand the largest exchange integral (corresponding to the largest sized crystals) is expected to yield the sharpest EPR line width of 10 mG. Between these extremes there are intermediate-sized crystals, which show a distribution of widths between these extremes. Thus the unusual shape of the EPR spectrum is due to the presence of crystals of various sizes in the mixture.

The above hypothesis was further confirmed by fitting the EPR spectrum obtained under anoxic conditions to a composite model of spin systems. The first-derivative experimental spectrum was fitted with a composite of n discrete line shapes corresponding to n different spin systems using the following expression that defines the line shape $Y(B)$ as a function of field:

$$Y(B) = \sum_{n=1}^{\infty} -2a_n^2(B - B_r)^2/b_n^2(1 + [(B - B_r)/b_n]^2)^2 \quad (3)$$

In the above expression, B_r is the resonance field, while a_n and b_n represent amplitude and width of the nth component. The parameters a and b were treated as variables to be evaluated for each component during fitting. Figure 1B shows the experimental and fitting data for a three-component system. It is observed that the experimental line shape is reproduced most closely with only three components suggesting that the system consists of three major components. The parameters—namely, line width and amplitude in the form of percent contribution (area) obtained in the fitting—are summarized in Table 1. The present results also explain the reporting of different values for the anoxic line width of LiPc in the literature. The anoxic line width of LiPc has been reported to be in the range from 5 to 60 mG.[13] Our results indicate that the difference in the reported widths is mostly due to differences in the crystal size used.

Effect of Oxygen on the EPR Line Width of LiPc. The EPR spectra obtained in the presence of various partial pressures of oxygen are shown in Figure 3. The peak-to-peak width

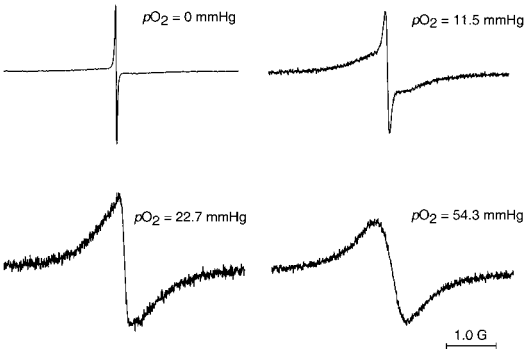

Figure 3. Effect of molecular oxygen on the EPR spectrum of microcrystalline LiPc at various partial pressures of oxygen. Experimental settings were as in Figure 1.

increases with oxygen and reaches a maximum value of about 650 mG. Similar increase in line width in the case of soluble probes such as nitroxides has been interpreted in view of the well-known Heisenberg spin-exchange with the molecular oxygen. However, in the case of solid-state probes such as LiPc, that has a low-dimensional spin diffusion, such a broadening is interpreted as due to the fixation of the mobile spins into fixed spins by the molecular oxygen.[19] When such a system is exposed to paramagnetic gases such as oxygen, the diffusing spins are trapped proportionate to the partial pressure of oxygen and converted into fixed spins. On increasing the partial pressure of oxygen the fraction of fixed spin to the mobile spin concentration is increased and thus the line width increases linearly with pO_2 initially. Beyond a certain value, typically when the equilibrium is reached, or in other words, all the diffusing spin states are trapped, further increase in pO_2 will not influence the EPR line width. This is quantitatively discussed in more detail later. This is in contrast to the generally observed linear variation of line width for all values of pO_2 in the case of soluble probes in solution phase. The observed LW as a function of pO_2 is shown in Figure 4A. The LW values in the figure were obtained as peak-to-peak widths of the composite spectra measured at the various pO_2 values. However, it is true that there are three components embedded into this spectrum. Detailed analyses of the component line shapes within the composite spectra are presented later. Figure 4A shows that saturation in LW is attained at pO_2 values higher that 50 mmHg. The highest value for LW obtained in the present study was 650 mG, at pO_2 about 100 mmHg, beyond which it became insensitive to oxygen. The maximum value of 650 mG also coincides with the value obtained for the amorphous form of LiPc. This means that in the presence of about 100 mmHg oxygen, all the mobile spins are converted into fixed spins and any further addition of oxygen is ineffective. Beyond this pO_2 no spin-exchange occurs and thus the microcrystals behave like the oxygen-insensitive amorphous material. It should be noted that such a nonlinear dependence of LW on pO_2 has also been observed in other solid probes such as biocompatible charcoal.[10]

The observation of a nonlinear behavior in the interaction of oxygen with LiPc, in the present study, is in contrast to the observation reported by Liu et al.[13a] They have observed a linear variation of line width with pO_2 values up to 800 mmHg. The present data also showed a higher slope 9.5 mG/mmHg, in the linear region of the response curve, while Liu et al. observed a slope of 6.1 mG/mmHg.[13a] These differences could be rationalized from a detailed analysis of the diffusion characteristics of molecular oxygen as a function of crystal size. The EPR line broadening in solution phase is governed by bimolecular collisions between the spin probe and molecular oxygen.

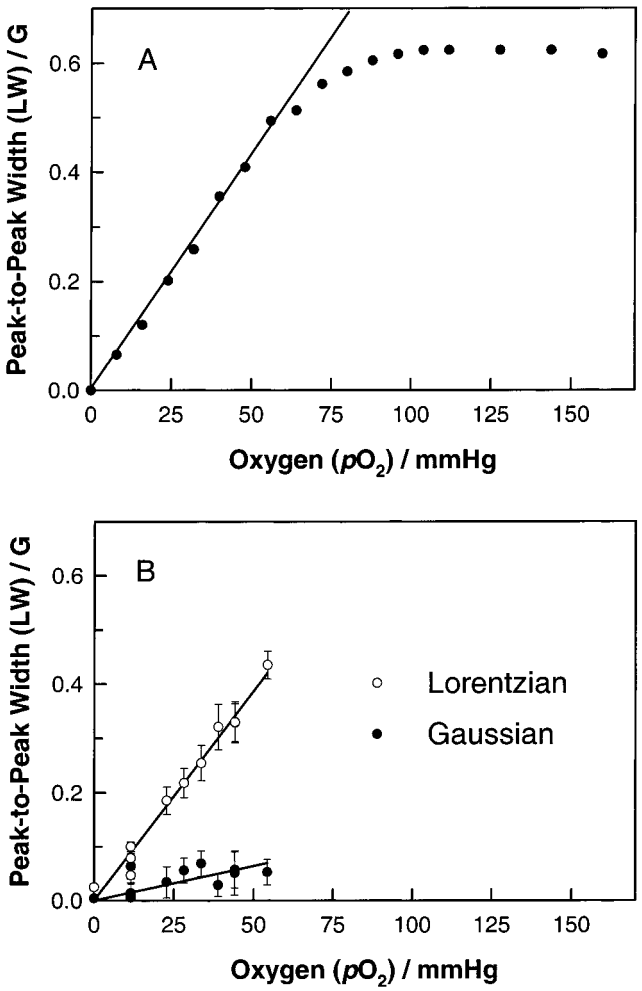

Figure 4. Effect of oxygen on the EPR line width of LiPc. (A) Peak-to-peak width (LW) of the spectrum as a function of oxygen partial pressure (pO_2). (B) Voigt shape analysis of the oxygen-broadened spectra. The deconvoluted Gaussian and Lorentzian widths of the experimental spectra show that the oxygen-induced broadening is predominantly Lorentzian in character, while the Gaussian broadening is smaller and invariant of oxygen.

According to the classical Smolukowski equation (eq 1), such a broadening is equally probable at any pO_2 and thus the broadening is expected to be linear with pO_2. However, the line broadening mechanism for a solid-state probe such as the LiPc is complex. The observation of a narrow line in LiPc is due to strong intermolecular spin exchange within the stack (intrastack exchange) as described in the previous section. The presence of oxygen affects the spin exchange within the stack (i.e., acts as trap), and subsequently the fixed spin (nonexchanging) concentration is increased, which leads to line broadening. At a given pO_2, the observed line width (LW) is defined as

$$\mathrm{LW} = c\,\mathrm{LW_f} + (1 - c)\mathrm{LW_m} \tag{4}$$

where LW_f and LW_m are the line widths in the fixed and the mobile spin states, c is the fraction of spin states converted from mobile state to the fixed state. As pO_2 increases, the fraction c increases proportionally, as described by the relationship $c = m\,pO_2$, where m is the proportionality constant.[17] Hence, as pO_2 is increased, the observed line width increases linearly as per eq 4. In any case, depending upon the nature of the material the proportionality constant m may vary, leading to a different slope of the straight line observed in the LW versus pO_2 plot. Actually, the slope of these plots directly reflects the sensitivity (or responsivity) of the probe to oxygen. The slope in the present work is observed to be twice the value reported for the LiPc single-crystal experiment.[13a] This is due to the fact that, in a microcrystalline sample consisting of small particles, oxygen can penetrate more easily and can more readily trap the mobile spins into fixed spins than a single crystal of higher dimension.

It is known[13e] that the x form of LiPc contains interstack channels (pores) with diameter of 6 Å. Since the dimension of molecular oxygen is 2.8 Å × 3.9 Å, it penetrates readily into the pore and subsequently perturbs the intrastack spin exchange. It is assumed that the oxygen diffuses through the channels without any significant adsorption. This assumption is based on the previous report where only diffusion of oxygen has been considered.[17] The diffusional flux of oxygen into the channels of LiPc can be visualized as flow of gaseous molecules into micropores. The nature of the flow is determined by the ratio of the pore radius (r) and the mean free path (λ) of the flowing gas.[20] Since the value of λ is much less than that of r for LiPc, the Knudsen's type of gas flow (where the probability of collision with pore walls is more than with other oxygen molecules) is more prominent. The Knudsen's diffusion coefficient (D_k) for tube with a circular cross section is defined as follows.[20]

$$D_k = 2ur/3 \tag{5}$$

Here, u is the mean molecular velocity defined as

$$u = (8RT/\pi M)^{1/2} \tag{6}$$

where M is the molecular weight. The Knudsen flux J_k is defined as[21]

$$J_k = D_k(\Delta pO_2)/(lRT) \tag{7}$$

where the ΔpO_2 is the pressure difference between the start and end of the pore and l is the length of pore. It is clear from the above expression that the oxygen flux, J_k, inside the pore inversely depends on the length of the pore, or in other words, on the length of the crystal. Thus, for a given pO_2 the fraction c of the fixed spin state also inversely depends on the crystal size. To summarize, the smaller the crystal size, the higher will be the concentration of the fixed spin states and hence the slope.The saturation behavior in the oxygen response curve can also be interpreted on the basis of the two-spin state model. As discussed above, when an LiPc crystal is exposed to oxygen the diffusing mobile spin states are converted into fixed states. Let n be the concentration of the total spin, pO_2 being the concentration of oxygen (the traps), ω_0 and the ω, the spin population for sites with and without oxygen, respectively. Now the concentrations of the fixed and the mobile spins, namely n_f and n_d, are given by the following equations:

$$n_f = nc = m(pO_2)\omega_0 \tag{8}$$

$$n_d = n(1 - c) = (1 - m(pO_2))\omega \tag{9}$$

The c in the above equations represents the fraction of total spin concentration converted into fixed state. Thus the relative concentration of the fixed spins can be expressed as[18,19]

$$c = m(pO_2)/[m(pO_2) + (1 - m(pO_2)(\omega/\omega_0))] \tag{10}$$

Now fraction c depends on two parameters, namely, the proportionality constant m and the ratio of population states ω/ω_0. The ω/ω_0 ratio is very critical and it determines the nature

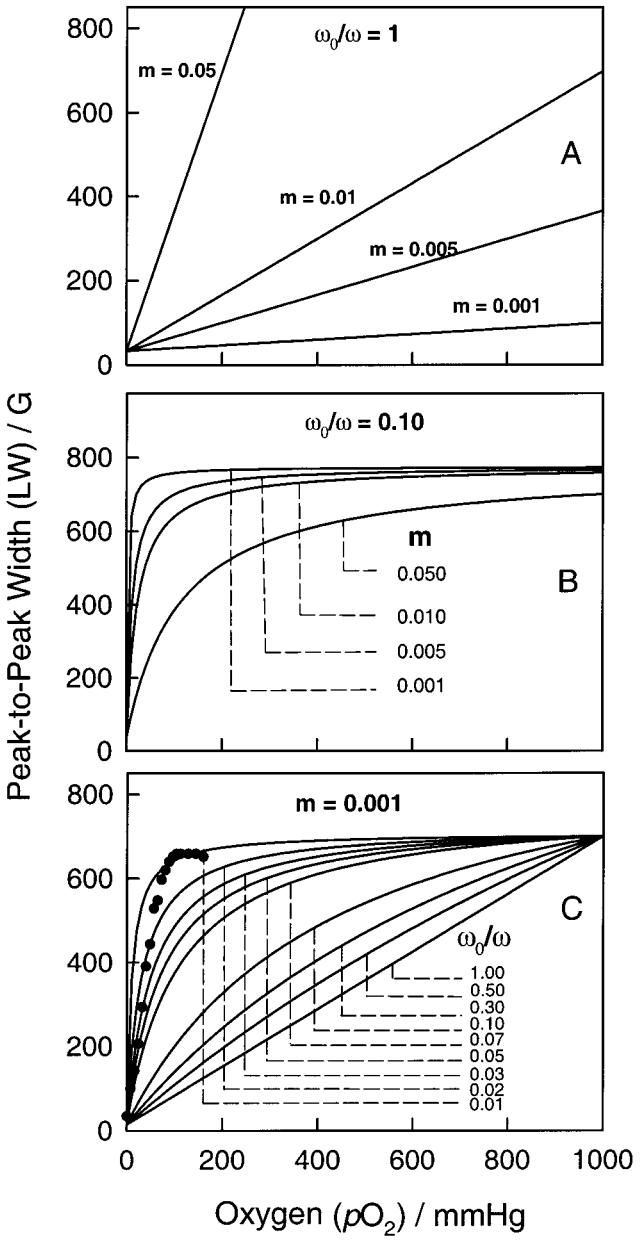

Figure 5. Simulated oxygen-response curves under various conditions. The curves were calculated using eqs 4 and 10 as described in the text. Response curves for various m values corresponding to $\omega_0/\omega = 1.0$ (A) and $\omega_0/\omega = 0.1$ (B) are shown. Panel C shows the response curves for various ω_0/ω values corresponding to $m = 0.001$. The solid circles represent the experimental line width data observed from the LiPc powder.

of the oxygen response curve. We carried out simulation of the oxygen response curves by combining eqs 4 and 10. We noticed that at any given ω/ω_0 value, the change in a value of the proportionality constant m altered the slope of the response curve, but the general shape of the curve remained the same (Figure 5A, B). On the other hand, the change in the ω/ω_0 ratio for a given value of m drastically changed the shape of the curve. Figure 5C illustrates the calculated oxygen response curves using eqs 4 and 10 for various ω/ω_0 values at $m = 0.001$. It is clear from the figure that the response curves tend to show curvature (saturation) as ω/ω_0 decreases. A linear variation is observed only when the ω/ω_0 is unity (Figure 5C).

According to the theory, at thermodynamic equilibrium, the ω/ω_0 is equal to $\exp(-E/kT)$, where E is the jumping energy from mobile state to fixed state and vice versa at any given temperature, T.[18] If the E is very small, then ω/ω_0 is close to one. This situation (i.e., $\omega \approx \omega_0$) becomes more probable when the total number of spin states, n, is very large so that even at high values of pO_2 a perfect equilibrium between the fixed and mobile spins is maintained. Hence, linearity in the response curve is maintained throughout the pO_2 range. This is the situation when one uses bigger crystals as probe. On the other hand, when E is large, the ω/ω_0 becomes smaller than unity and the lower ω/ω_0 values lead to the steep rise and saturation at higher pO_2 as described in Figure 5C. This is the case where one uses smaller crystals and hence even smaller pO_2 can largely change the ω/ω_0 ratio. Another important inference from the Figure 5C is that for larger crystals, though the linear region is observed for wide range of pO_2, the slope is smaller and thus the sensitivity. On the other hand for smaller crystals, the linear region is limited to lower pO_2 but the sensitivity is higher. This explains why the sensitivity is considerably higher for the microcrystalline powder of the present case than reported previously for single crystals.[13a] The Figure 5C also contains the experimental line width data measured at various pO_2. The data do not confine to any single line and it merges with at least four theoretical lines. This suggests that the sample may have crystals of at least three or four different sizes (and correspondingly four different ω/ω_0). When a mixture of crystals of various sizes is exposed to oxygen, the smallest crystal responds first. This result also substantiates the prediction in the previous section that the spin dynamics depends on the size of the crystals. The experimental data shown in Figure 4 is also in consistent with this prediction.

Another interesting aspect observed in the EPR spectra of LiPc in the presence of molecular oxygen is the change of line shape. While the EPR line in the case of anoxic conditions could be described by a Lorentzian function, the line shape in the presence of oxygen could be described only by a Voigt-type function, which is a combination of both Gaussian and Lorentzian functions.[1] A thorough discussion and justification of the use of Voigt function for an inhomogeneously broadened line due to the increase in transverse relaxation time T_2, is available.[21] When the EPR spectra obtained at various pO_2 were analyzed using the Voigt line shape expression, we found that the Gaussian width remained small and constant while the Lorentzian line width increased with pO_2 as illustrated in Figure 4B. This observation is also consistent with the earlier reports on oximetry based on soluble probes.[9] Thus, though the line broadening mechanism is different in the case of LiPc, the EPR line shape characteristics are the same as in the case of soluble probes.

To substantiate our interpretation that the oxygen response curve of LiPc depends on the particle size, we performed fitting of the EPR spectra obtained at various pO_2 using the Voigt functions considering three lines as discussed above (Figure 1B). The analysis was restricted to the pO_2 range corresponding to the linear region of the response curve seen in Figure 4A. For all the three lines the LW increased with pO_2 but to different extents. The Lorentzian line widths obtained from such analysis are plotted in Figure 6. Also the proportionality constant m, which reflects the slope of the oxygen response curve, are summarized in Table 1. As can be seen in Figure 6, the smaller crystals, giving LW about 70 mG in anoxic conditions, showed higher m but saturated in very low pO_2 itself, which is about 20 mmHg. On the other hand, the largest crystals with <10 mG line width showed smaller m but maintained the linearity throughout the region.

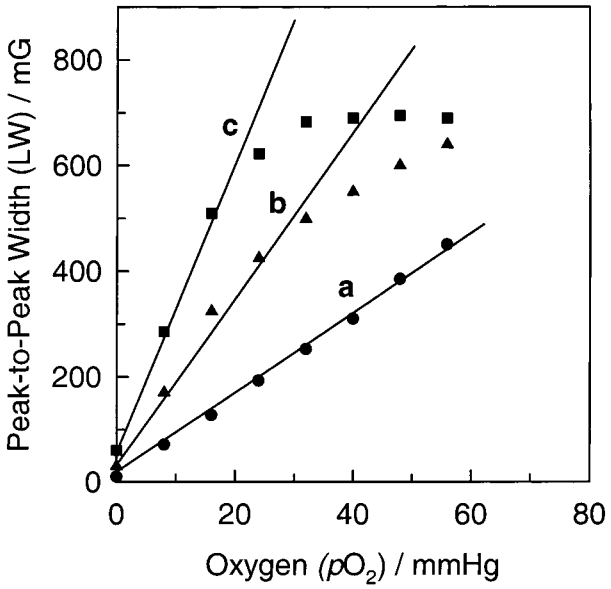

Figure 6. Decomposed oxygen-response curves obtained from experimental data. The response curves a, b, and c correspond to the three major components (Figure 1B and Table 1) present in the EPR spectrum of the LiPc microcrystalline powder. It is seen that the components respond to oxygen to different extents.

Summary and Conclusions

This study demonstrates the involvement of several important factors on the use of the LiPc crystals as EPR oximetry probes to estimate oxygen in any chemical/biological system. The size of the particle is the most important factor since the oxygen flow in to the channels can be severely influenced by the size. The calibration curve must be constructed under similar experimental conditions. More importantly, the size of the crystals used in the experiment should be in the same order as that used to construct the calibration curve. Any discrepancy in size can potentially introduce considerable amount of error in the measurements. As the size of the crystal decreases, the sensitivity of the method is dramatically increased, while the linear variation range is compromised at lower pO_2 values. On the other hand, with larger crystals, the oxygen sensitivity is decreased but the dynamic working range of line broadening is increased. Thus depending upon the application requirement, one can choose different crystal sizes. For example, an oxygen measurement in pathophysiology like ischemia where the change in the pO_2 can vary between 0.1 and 150 mmHg,[14] the microcrystalline particulate system is very appropriate with very high sensitivity. For systems where the pO_2 is higher such as hyperoxic exposed, one has to use bigger crystals. When the EPR of the crystalline mixture is obtained under anoxic conditions, the resultant spectrum has many components corresponding to different sizes. The EPR line width in the absence of oxygen depends on the size of the crystal due to the different magnitude of spin exchange.

Acknowledgment. We acknowledge the financial support from the National Cancer Institute (NIH) Grant CA 78886, NIH Grants GM 58582 and RR 12190, and the Alexander and Margaret Stewart Trust. P.K. was supported by the Established Investigator Award from the American Heart Association during the tenure of this work.

References and Notes

(1) Ardenkjaer-Larsen, J. H.; Laursen, I.; Leunbach, I.; Ehnholm, G.; Wistrand, L.-G.; Peterson, J. S.; Golman, K. *J. Magn. Reson.* **1998**, *133*, 1.

(2) Hwang, J.-T.; Greenberg, M. M.; Fuchs, T.; Gates, K. S. *Biochemistry* **1999**, *38*, 14248.

(3) (a) Belkin, S.; Mehlhorn, R. J.; Packer, L. *Arch. Biochem. Biophys.* **1987**, *252*, 487. (b) Strzalka, K.; Sarna, T.; Hyde, J. S. *Photobiochem. Photobiophys.* **1986**, *12*, 67.

(4) Kalyanaraman, B.; Feix, J. B.; Sieber, F.; Thomas, J. P.; Girotti, A. W. *Proc. Natl. Acad. Sci. U.S.A.* **1987**, *84*, 2999.

(5) Hyde, J.; Subczynski, W. K. Spin Label Oximetry. In *Biological Magnetic Resonance*; Berliner, L. J., Ranlen, J., Ed.; Plenum: New York, 1989; Vol. 8, p 399.

(6) (a) Stehling, M. K.; Schmitt, F.; Ladebeck, R. *J. Magn. Reson. Imaging* **1993**, *3*, 471. (b) Shukla, H. P.; Mason, R. P.; Woessner, D. E.; Antich, P. P. *J. Magn. Reson. B* **1995**, *106*, 131.

(7) Grucker, D.; Chambron, J. *Magn. Reson. Imaging* **1993**, *11*, 691.

(8) Kuppusamy, P.; Chzhan, M.; Vij, K.; Shteynbuk, M.; Lefer, D. J.; Giannella, E.; Zweier, J. L. *Proc. Natl. Acad. Sci. U.S.A.* **1993**, *91*, 3388. (b) Sendhil Velan, S.; Spencer, R. G. S.; Zweier, J. L.; Kuppusamy, P. *Magn. Reson. Med.* **2000**, *43*, 804.

(9) Swartz, H. M.; Glockner, J. F. In *EPR Imaging and in vivo EPR*; Eaton, G. R., Eaton, S. S., Ohno, K., Eds.; CRC Press: Boka Raton, FL, 1991.

(10) He, G.; Shankar, R. A.; Chzhan, M.; Samouilov, A.; Kuppusamy, P.; Zweier, J. L. *Proc. Natl. Acad. Sci. U.S.A.* **1999**, *96*, 4586.

(11) (a) Vahidi, N.; Clarkson, B.; Liu, K. J.; Norby, S. W.; Wu, M.; Swartz, H. M. *Magn. Reson. Med.* **1994**, *31*, 139. (b) James, P. E.; Grindberg, O. Y.; Goda, F.; Panz, T.; O·Hara, T.; Swartz, H. M. *Magn. Reson. Med.* **1997**, *37*, 48.

(12) (a) Goda, F.; Liu, K. J.; Walczak, T.; O·Hara, J. A.; Jiang, J.; Swartz, H. M. *Magn. Reson. Med.* **1995**, *33*, 237. (b). Swartz, H. M.; Liu, K. J.; Goda, F.; Walczak, T. *Magn. Reson. Med.* **1994**, *31*, 229.

(13) (a) Liu, K. J.; Gast, P.; Moussavi, M.; Norby, S. W.; Vahidi, N.; Walczak, T.; Wu, M.; Swartz, H. M. *Proc. Natl. Acad. Sci. U.S.A.* **1993**, *90*, 5438. (b) Liu, K. J.; Bacic, G.; Hoopes, P. J.; Jiang, J.; Du, H.; Ou, L. C.; Dunn, J. F.; Swartz, H. M. *Brain Res.* **1995**, *685*, 91. (c) Afeworki, M.; Miller, N. R.; Devasahayam, N.; Cook, J.; Mitchell, J. B.; Subramanian, S.; Krishna, M. C. *Free Rad. Biol., Med.* **1998**, *25*, 72. (d) Brinkmann, M.; Andre, J.-J.; *J. Mater. Chem.* **1999**, *9*, 1511. (e) Ilangovan, G.; Zweier, J. L.; Kuppusamy, P. *J. Phy. Chem. B* **2000**, *104*, 4047.

(14) Zweier, J. L.; Chzhan, M.; Ewert, U.; Schneider, G.; Kuppusamy, P., *J. Magn. Reson.* **1994**, *B105*, 52.

(15) Weil, J. A.; Bolton, J. R.; Wertz, J. E. *Electron Paramagnetic Resonance. Elementary Theory and Practical Applications*; John Wiley: New York, 1994.

(16) Smirnov, A. I.; Norby, S.-W.; Walczak, T.; Liu, K. J.; Swartz, H. M. *J. Magn. Reson. B* **1994**, *103*, 95.

(17) Benseba, F.; Andre, J. J. *J. Phys. Chem.* **1992**, *96*, 5739.

(18) Holzer, K.; Boucher, J. P.; Devreux, F.; Nechtschein, M. *Phys. Rev.* **1981**, *23*, 1051.

(19) Nechtschein, M.; Devreux, F.; Genoud, F.; Guglielmi, M.; Holczer, K. *Phys. Rev.* **1983**, *27*, 61.

(20) Frank-Kamenetskii, D. A. *Diffusion and Heat Transfer in Chemical Kinetics*, 2nd ed.; Plenum Press: New York, 1969.

(21) Bales, B. L. Inhomogeneously Broadened Spin-Label Spectra. In *Biological Magnetic Resonance. Spin Labeling. Theory and Applications*; Berliner, L., Reuben, J., Eds.; Plenum: New York, 1989; Vol. 8, p 77.